Physics-informed Machine Learning for Parameter Estimation of DC-DC Converter

Shuai Zhao, Yingzhou Peng, Yi Zhang, and Huai Wang
Department of Energy
Aalborg University, Aalborg 9220, Denmark
Email: {szh, ype, yiz, hwa}@energy.aau.dk

2022 IEEE Applied Power Electronics Conference and Exposition (APEC) | 978-1-6654-0688-8/22/$31.00 ©2022 IEEE | DOI: 10.1109/APEC43599.2022.9773482

***Abstract*—Although various machine learning-based methods have been proposed for condition monitoring in power electronics, they are challenging to be implemented in practice due to the accuracy, data availability, computation burden, explainability, etc. Physics-informed machine learning (PIML) has been emerging as a promising direction where the above challenges can be mitigated by incorporating domain knowledge. In this paper, we propose a PIML-based parameter estimation method for a DC-DC Buck converter, as an exemplary application of PIML in power electronics. By seamlessly integrating a deep neural network and the converter physical model, it can estimate multiple component parameters simultaneously with high accuracy and robustness, while based on a limited dataset. It expects to provide a new perspective to tailor existing ML tools for power electronic applications.**

I. Introduction

Accurate monitoring of the parameter variations of key components (e.g., power semiconductor devices, capacitors, etc.) is essential for prognostics and health management of power electronic systems [1]. For industry applications, non-invasive condition monitoring approaches assisted by machine learning (ML) are favorable as they require no extra hardware sensors. For this topic, numerous ML-assisted data-driven parameter estimation methods have been reported in the literature [2], [3]. For example, in [4], the nonlinear relationship between the capacitance of the DC-link capacitor and the harmonics of the DC-link ripple voltage is modeled by using a feed-forward neural network. With the well-trained feed-forward neural network, the capacitance can be indirectly inferred from the harmonics of ripple voltage without extra hardware. To monitor the capacitor aging in DC filters, in [5], an adaptive neuro-fuzzy inference system algorithm is trained to establish the functional relationship between the inputs including the converter input voltage and voltage crossing the DC filters, and the output as the capacitor aging index in the DC filters. As a result, the capacitor aging index can be indirectly accessed with the existing voltage information. However, most previous studies are challenging to be implemented in practice due to several common limitations [6]. First, the training dataset for the machine learning approaches is challenging to prepare [7] as it requires, e.g., perturbation of control signals, high sampling frequency, extra sensors, large/diversified dataset, etc. Second, given the same input data, the algorithm robustness and repeatability [3] are not acceptable for industrial applications due to the poor accountability and explainability of ML methods. Third, for the unexplored cases with few data [4] during the training stage, the model's generalization capability is worse resulting in poor prediction accuracy.

Physics-informed machine learning (PIML) is gaining widespread attention nowadays [8]–[10]. In contrast to conventional ML methods purely driven by the data, PIML is focusing on how to exploit physical models to ease the data-driven pipeline using the machine learning. To date, the PIML tools have achieved success in complex engineering fields such as fluid mechanics [11], power systems [12], etc. Considering the well-established physical models in power electronics, this paper proposes a new parameter estimation method for power electronic systems with PIML. Specifically, the physical model of a DC-DC Buck converter is seamlessly coupled into the training of deep neural network to mitigate the common challenges existed in data-driven condition monitoring. We found that the PIML-based parameter estimation method is accurate and robust, while without extensive and trivial training data collection. As for the data-light feature, its implementation on the DC-DC Buck converter only requires a small number of peak values of the inductor current and output voltage. Moreover, in principle, the method is generic and scalable to complex power electronic systems with a larger number of parameters.

The remainder of this paper is organized as follows. Section II presents the system dynamic model of a DC-DC Buck converter, the idea of the physics-informed neural network for parameter estimation for general dynamic systems, and the implementation of physics-informed neural network for its parameter estimation of the DC-DC Buck converter. In Section III, both the simulation and the hardware experiments are conducted for the method verification. Finally, Section IV concludes the paper.

II. Parameter Estimation with Physics-informed Machine Learning

In this paper, a DC-DC Buck converter is applied as an exemplary application to illustrate the PIML-enabled parameter estimation method in power electronics. DC-DC Buck converter is a fundamental circuit in power electronic applications. The circuit topology of a DC-DC Buck converter is given in Fig. 1, and its physical dynamic model can be formulated with differential equations as (1):

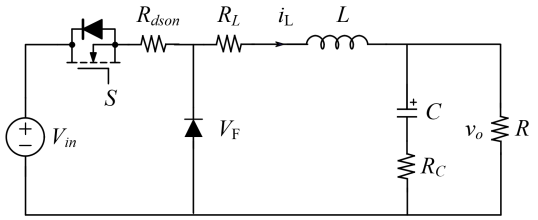

Fig. 1. The circuit topology of a DC-DC Buck converter.

$$\begin{bmatrix} \frac{di_L}{dt} \\ \frac{dv_C}{dt} \\ v_o \end{bmatrix} = \begin{bmatrix} -\frac{A}{L} & -\frac{1}{L}(\frac{R}{R_C+R}) \\ \frac{1}{C}(\frac{R}{R_C+R}) & -\frac{1}{C}(\frac{1}{R_C+R}) \\ \frac{R_C R}{R_C+R} & \frac{R}{R_C+R} \end{bmatrix} \times \begin{bmatrix} i_L \\ v_C \end{bmatrix} + S \begin{bmatrix} \frac{v_{in}}{L} \\ 0 \\ 0 \end{bmatrix} + (1-S) \begin{bmatrix} \frac{-V_F}{L} \\ 0 \\ 0 \end{bmatrix}, \tag{1}$$

where $A = (S \cdot R_{dson} + R_L + (R_C R)/(R_C + R))$. S is the state of the power semiconductor device that is 1 when it is ON or 0 otherwise. i_L is the inductor current, v_C is the DC capacitor voltage, v_o is the output voltage, R_L is the load resistance, R_{dson} is the on-state resistance of the power semiconductor device, C is the capacitance, and R_C is its equivalent series resistance (ESR). V_{in} is the input voltage and V_F is the diode forward voltage. For the parameter estimation task of (1), it aims to estimate the component parameters (e.g., the capacitance C, the ESR R_C, etc.) based on the easily accessible data i_L and v_o. In essence, it is an inverse task of differential equations. Although there are several numerical solvers for the inverse tasks in literature, they are not practical here due to the distinctive features of the condition monitoring applications on power electronic systems [3], e.g., system stiffness behavior, data sparsity, data noise, high accuracy requirement, etc.

In [10], a deep neural network is applied to the parameter estimation and the prediction tasks of differential equations, formulated as a specific physics-informed neural network (PINN). The PIML tool has been demonstrated on several classical differential equation problems (e.g., Navier–Stokes equation, Schrodinger equation, etc.). It indicates that the PIML method is efficient and robust to tackle the parameter estimation and prediction tasks, especially in the presence of noise, sparsity, and limited datasets. Specifically, consider a general dynamic system governed by the differential equations:

$$u_t + \mathcal{N}[u;\lambda] = 0, x \in \Omega, t \in [0,T], \tag{2}$$

and define the physical constraints f as

$$f := u_t + \mathcal{N}[u;\lambda], \tag{3}$$

where $u = u(\boldsymbol{x}, t)$ denotes the solution/data of differential equations, $\boldsymbol{x}$ are the space coordinates, and t is the time coordinate. Suppose that the system is observed with the state $u(t_n)$ at the time t_n and the state $u(t_{n+1})$ at the time t_{n+1}, where $t_{n+1} = t_n + \Delta t$. Meanwhile, in addition to the observable states $u(t_n)$ and $u(t_{n+1})$, assume that the dynamic system will go through q intermediate states $u(t_{n+c_i})$, $i = 1, ..., q$, during the Δt time period, where $t_{n+c_i} = t_n + c_i \Delta t$, $c_i \in [0, 1]$. Note that these intermediate states are unobservable. According to [10], by using the framework of the implicit Runge-Kutta (IRK) method, the observable states $u(t_n)$ and $u(t_{n+1})$ and the intermediate states $u(t_{n+c_i})$ can be explicitly coupled with $q-$stages IRK method [13], through the backward equation (4) and forward equation (5):

$$u_i(t_n) = u(t_{n+c_i}) + \Delta t \sum_{j=1}^{q} a_{ij} \mathcal{N}[u(t_{n+c_j});\lambda], \tag{4}$$

and

$$u_i(t_{n+1}) = u(t_{n+c_i}) + \Delta t \sum_{j=1}^{q} (a_{ij} - b_j) \mathcal{N}[u(t_{n+c_j});\lambda]. \tag{5}$$

where $i, j = 1, ..., q$, $u_i(t_n) = u(t_n)$, and $u_i(t_{n+1}) = u(t_{n+1})$. The parameter set $\{a_{ij}, b_j, c_j\}$ can be determined given a certain step number q in the implicit Runge–Kutta method, as a Butcher tableau [13]. As a result, the relationship between the data $u(t_n)$, $u(t_{n+1})$, and the intermediate unobservable states $u(t_{n+c_i})$ are governed by the backward and forward equations, which can embed the unknown system parameters λ in $\mathcal{N}[\cdot]$. Meanwhile, considering the universal approximation capability of neural network, a deep neural network is applied to approximate q intermediate states $u(t_{n+c_i})$. With the observable data $u(t_n)$, $u(t_{n+1})$ and the approximated intermediate states $u(t_{n+c_i})$, the parameters λ can be obtained by training the neural network.

Likewise, such a configuration is applied to the parameter estimation of a DC-DC Buck converter in this paper. Specifically, the PIML-enabled parameter estimation is given in Fig. 2. The training data for the PIML is selected as the peak values of the inductor current and output voltage for the transient signals, as these data are more informative and sensitive to the converter parameter variations. There are two dynamic terms in the physical model (1), i.e., the inductor current and the output voltage. Take the inductor current as an example. Suppose that it is only available at peak points of each switching period, i.e., the lower peak current $i_L(t_n)$ and upper peak current $i_L(t_{n+1})$. The time between the two points is denoted as Δt, i.e., $t_{n+1} = t_n + \Delta t$. Also,

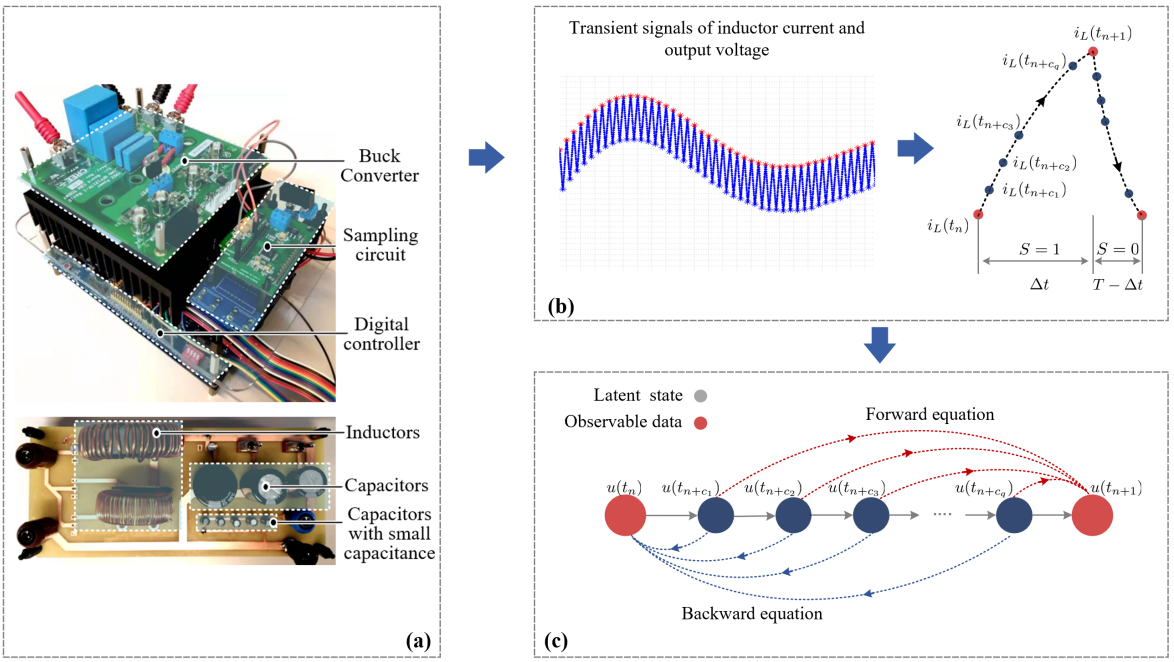

Fig. 2. Flowchart of physics-informed machine learning method for parameter estimation of a Buck converter. (a) the designed hardware experimental prototype; (b) the peak values of the transient signals of the inductor current and output voltage are used as the training data; and (c) the physical model of (1) is derived as the backward equation (4) and the forward equation (5) to establish the relationships between $i_L(t_n)$ and $i_L(t_{n+1})$ with latent states $i_L(t_{n+c_k})$, $k = 1, ..., q$.

suppose that the intermediate states between the peak current points are $i_L(t_{n+c_k})$, $k = 1, ..., q$, $c_k \in [0, \Delta t]$. It is worth mentioning that these intermediate states are unobservable. From a dynamic system perspective, given the initial condition $i_L(t_n)$, the converter is expected to cross each latent states $i_L(t_{n+c_k})$, respectively, and finally reach the state $i_L(t_{n+1})$ during the Δt time. Based on (1), the latent states $i_L(t_{n+c_k})$ can be used to bridge the relationship between $i_L(t_n)$ and $i_L(t_{n+1})$ with backward equation (4) and forward equation (5), respectively, by substantiating the general form (2) with the physical model (1) of the converter. The above analysis is applied to the output voltage v_o as well.

For the parameter estimation procedure, specifically, a physics-informed neural network consisting of a data-driven part and a physical model part, is applied to characterize the dynamics of the inductor current and output voltage in (1), and the method structure is shown in Fig. 3. The data-driven part is facilitated with a deep neural network, by exploiting the strong universal approximation capability of deep learning. The deep neural network inputs include the initials of inductor current i_L and output voltage v_o, the switch state S, and the Δt time from the initial to end. As a result, this deep neural network is designed to construct and approximate the intermediate states $[i_L(t_{n+c_1}), \ldots, i_L(t_{n+c_q}), v_o(t_{n+c_1}), \ldots, v_o(t_{n+c_q})]$, as its outputs. Subsequently, they are used as the prior information for the physical model part. For the physical model part, a q-steps implicit Runge-Kutta time-stepping scheme [10] is applied to construct the relationship between $i_L(t_n)$ and $i_L(t_{n+1})$, through backward and forward equations in the IRK framework based on the physical model (1), which involves all the unknown converter parameters (e.g., R_L, C, R_C, v_{in}, v_F, etc.) in (1) during the ML training stage. In this design, the data-driven part and physical model part are seamlessly integrated. Through the training of PINN, the unknown parameters in (1) can be learned together with the neuron weights $\mathbf{W}$ and biases $\mathbf{b}$ in the data-driven part, by using standard neural training methods, e.g., backpropagation training scheme. Also, in most cases, it is worth mentioning that there are thousands of parameters in the data-driven part. Since the system parameters in the physical parts are estimated with that in the data-driven part simultaneously, there is no limitation on the number of system parameters in the physical model, indicating the method scalability. In this way, the PINN learns the nonlinear and dynamic behavior of the DC-DC Buck converter system in a period Δt, through a supervised learning task.

III. Simulation and Hardware Testing

In this section, the proposed method is demonstrated both on simulation data and experimental data based on the designed hardware of a DC-DC Buck converter, as shown in Fig. 2 (a). The simulated converter is implemented in Matlab. It is set to regulate the DC voltage from 24 V to 9 V, with the switching frequency $f_{sw} = 20$ kHz. For the simulation data collection, only the peak values of the inductor current and output voltage when transient behavior occurs due to arbitrary workload changes (e.g., $R_1 \to R_2$, $R_2 \to R_3$, $R_3 \to R_1$, etc.) are used. One example of the transient signals are given in Fig. 2 (b)). Such a dataset can be easily accessed and prepared in

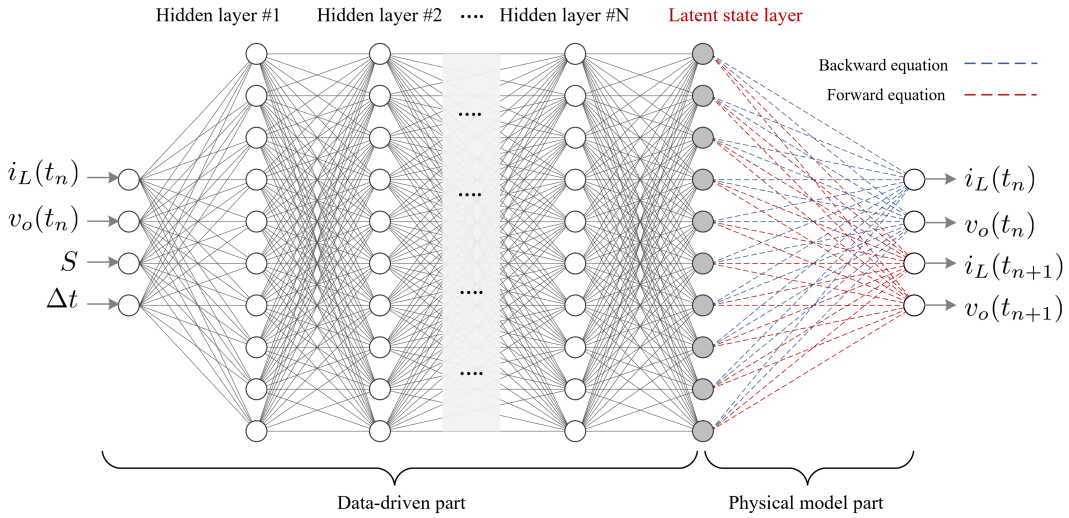

Fig. 3. The physics-informed neural network structure for the parameter estimation of the DC-DC Buck Converter. The backward and forward equations are given in (4) and (5), respectively, by substantiating with the physical model of the DC-DC Buck converter in (1).

the industrial applications. For example, the transient signals of the traction inverter in the railway applications can be readily collected during the train acceleration or deceleration. During the workload changes, only a total of 200 data pairs $\{i_L(t_n) \leftrightarrow i_L(t_{n+1}), v_o(t_n) \leftrightarrow v_o(t_{n+1})\}$ are collected for the PINN training. To ensure the sufficient expressivity of the neural network in approximating the intermediate states, a deep neural network with 4 layers with 50 neurons in each layer is applied in the data-driven part. The IRK time-stepping stage is set as q=20, considering the machine precision [10] and the time Δt. The deep neural network is firstly trained by using the Adam optimizer, with the default parameter settings (the learning rate $\eta = 0.001$, exponential decay rates $\beta_1 = 0.9$ and $\beta_2 = 0.999$). The epoch of the Adam optimizer is set as 200000. Afterward, it is further trained by using a full-batch optimizer L-BFGS [10].

Note that one of the main differences between data collected in the simulation setting and the hardware setting lies in the external disturbance factors. In addition to the directly simulated clean data, we have also manually injected external disturbance factors to emulate the data collected from the practical cases, to verify the method robustness. The external factors include the synchronization error between i_L and v_o (random sync error of 0-1μs is added), different levels of external noise (standard derivation of 1x random noise of current is 1.5 mA $(6/(2^{12}-1))$ and that of voltage is 2.9 mV $(12/(2^{12}-1))$), ADC quantization error (12-bit ADC is used to quantize the signal).

Table I shows the percentage error of parameter estimation results based on the simulation data. Based on this limited dataset, it can be seen that the estimation errors of all parameters are less than 0.2% in the clean data testing case, which suggests the proposed method can provide an accurate estimation. Meanwhile, when adding the disturbance factors of different levels of noise, ADC quantization error, and synchronization error, the estimation accuracy decreases in a limited scope, which suggests that the proposed method is robust in terms of the external noise, ADC quantization error, and synchronization error. Note that the estimation results of R_L and R_{dson} are less accurate compared to other parameters. While compared to the individual R_L and R_{dson}, it can be seen that the sum of R_L and R_{dson} as R_{L+dson} is more accurate and stable in terms of different affecting factors. As a result, the indicator R_{L+dson} is chosen for the condition monitoring of the inductor and power semiconductor device together, which is aligned with the fact found in [3] as well.

Likewise, the proposed method is also experimentally verified and the data collection procedure is the same as the simulation data. A hardware platform of a DC-DC Buck converter is developed to verify the proposed method in field applications, as shown in Fig. 2.(a). This testing platform is based on our previous work [3], where the capacitor and power semiconductor device can be easily replaced to emulate the device degradation behavior. It regulates the DC voltage from 48 V to 24 V. Specifically, the two most vulnerable components in the DC-DC Buck converter including the power semiconductor devices (three different devices denoted as M1: 0.225 Ω, M2: 0.152 Ω, M3: 0.072 Ω) and capacitors (four different devices denoted as C1: 164.5 μF, C2: 160.7 μF, C3: 156.8 μF, C4: 152.9 μF) are manually changed to simulate the degradation behaviors, forming different testing groups (e.g., C1M1). As the benchmark value, the degradation percentage is shown with blue points in Fig. 4. For each testing group, the transient signals are independently collected three times to verify the method repeatability. The parameter estimation error of each testing case is shown with the green bar and the mean of the testing group is shown with the red bar. For each testing group, it is noted that the estimation difference of the three testing cases is almost negligible, indicating the proposed method can provide stable results with good

Table I: Percentage error (%) of simulation analysis for different testing cases (ADC: ADC quantization error; Sync error: Synchronization error). All the results below 0.1% are rounding up to 0.1% for clarity.

Error (%) / Testing cases	L	R_L	C	R_C	R_{dson}	R_{L+dson}	R_1	R_2	R_3	V_{in}	V_F
Clean data	0.1	0.1	0.1	0.1	0.2	0.1	0.1	0.1	0.1	0.1	0.1
1x noise-ADC-Sync error	0.1	1.7	0.1	0.1	4.8	0.5	0.1	0.1	0.1	0.1	1.0
5x noise-ADC-Sync error	0.5	9.1	0.1	0.2	24.1	2.1	0.1	0.2	0.2	0.4	4.5
10x noise-ADC-Sync error	1.0	15.6	1.9	0.6	48.8	6.0	0.1	0.1	0.1	0.4	1.0

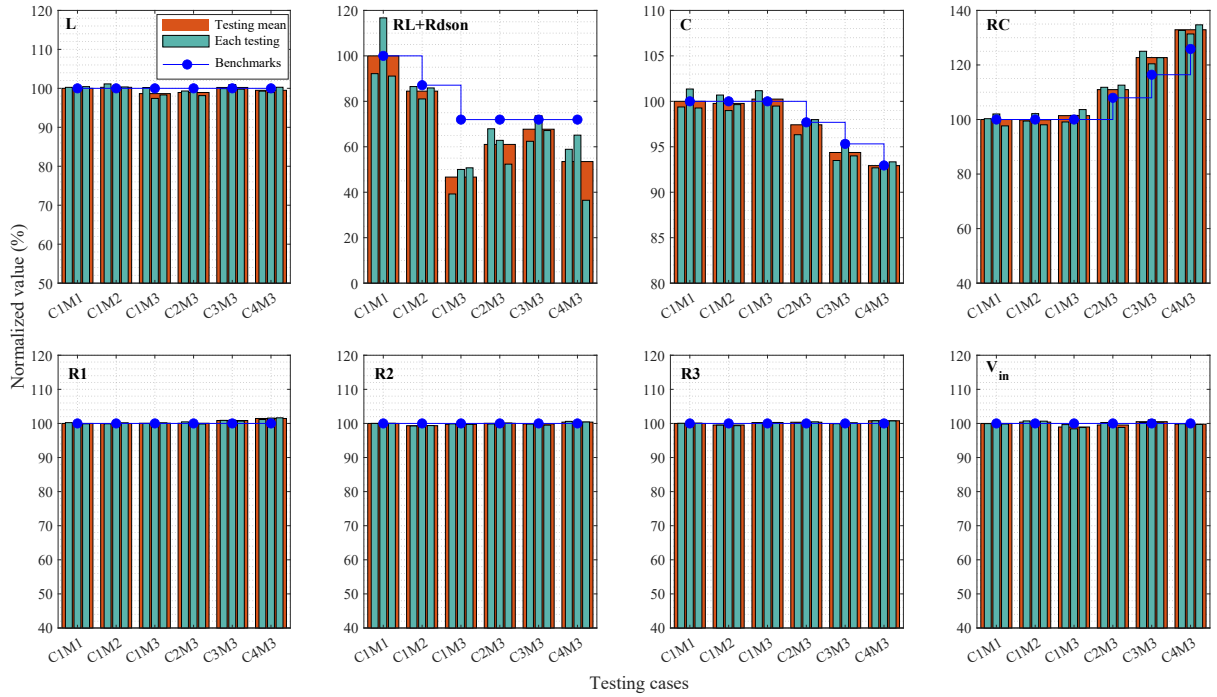

Fig. 4. Hardware testing results of PINN-based parameter estimation for DC-DC Buck converter. The results of each testing group are normalized in terms of the benchmark group C1M1.

repeatability. Also, the parameter variation percentage is very close to the benchmark values. It is worth mentioning that the relatively large error of R_{dson} and R_L is due to the fact that the two components (e.g., R_{dson} and R_L) in the physical model (1) are only applied as the constant unknown variables. Nevertheless, in the field operation, R_{dson} is highly affected by the operational conditions, e.g., temperature, current, etc., and those factors have not been considered in the converter physical model (1). Moreover, the R_L may be varied with different inductor current i_L, which is neglected in the model as well. Thus, more investigations are required to improve the fidelity of the converter physical model in future works.

IV. Conclusions

In this paper, a physics-informed machine learning-enabled parameter estimation is proposed for a DC-DC Buck converter. As demonstrated both in the simulation and hardware testing, integrating the physical model of the DC-DC Buck converter with the deep neural network enables a highly accurate and robust parameter estimation, while requiring a limited dataset of only 200 data pairs. The three common challenges in purely data-driven parameter estimation can be addressed in the proposed method, which indicates the benefits of integrating physical knowledge and ML tools for condition monitoring in power electronics.

References

[1] S. Zhao and H. Wang, "Enabling data-driven condition monitoring of power electronic systems with artificial intelligence: Concepts, tools, and developments," *IEEE Power Electron. Mag.*, vol. 8, no. 1, pp. 18–27, Mar. 2021.

[2] M. Al-Greer, M. Armstrong, M. Ahmeid, and D. Giaouris, "Advances on system identification techniques for dc-dc switch mode power converter applications," *IEEE Trans. Power Electron.*, vol. 34, no. 7, pp. 6973–6990, Oct. 2019.

[3] Y. Z. Peng, S. Zhao, and H. Wang, "A digital twin based estimation method for health indicators of dc-dc converters," *IEEE Trans. Power Electron.*, vol. 36, no. 2, pp. 2105–2118, Jul. 2021.

[4] H. Soliman, I. Abdelsalam, H. Wang, and F. Blaabjerg, "Artificial neural network based DC-link capacitance estimation in a diode-bridge front-end inverter system," in *IEEE 3rd Int. Future Energy Electron. Conf. ECCE Asia*, 2017, pp. 196–201.

[5] T. Kamel, Y. Biletskiy, and L. Chang, "Capacitor aging detection for the dc filters in the power electronic converters using ANFIS algorithm," in *IEEE 28th Canadian Conf. Elect. Comput. Eng. (CCECE)*, 2015, pp. 663–668.

[6] S. Zhao, F. Blaabjerg, and H. Wang, "An overview of artificial intelligence applications for power electronics," *IEEE Trans. Power Electron.*, vol. 36, no. 4, pp. 4633–4658, Apr. 2021.
[7] B. X. Li and K. S. Low, "Low sampling rate online parameters monitoring of dc-dc converters for predictive-maintenance using biogeography-based optimization," *IEEE Trans. Power Electron.*, vol. 31, no. 4, pp. 2870–2879, Apr. 2016.
[8] K. E. Willcox, O. Ghattas, and P. Heimbach, "The imperative of physics-based modeling and inverse theory in computational science," *Nature Computational Science*, vol. 1, no. 3, pp. 166–168, Mar. 2021.
[9] G. E. Karniadakis, I. G. Kevrekidis, L. Lu, P. Perdikaris, S. Wang, and L. Yang, "Physics-informed machine learning," *Nature Reviews Physics*, vol. 3, no. 6, pp. 422–440, May 2021.
[10] M. Raissi, P. Perdikaris, and G. E. Karniadakis, "Physics-informed neural networks: A deep learning framework for solving forward and inverse problems involving nonlinear partial differential equations," *J. Computational Physics*, vol. 378, pp. 686–707, Feb. 2019.
[11] M. Raissi, A. Yazdani, and G. E. Karniadakis, "Hidden fluid mechanics: Learning velocity and pressure fields from flow visualizations," *Science*, vol. 367, no. 6481, pp. 1026–1030, Feb. 2020.
[12] G. S. Misyris, A. Venzke, and S. Chatzivasileiadis, "Physics-informed neural networks for power systems," in *IEEE Power & Energy Soc. General Meeting (PESGM)*, 2020, pp. 1–5.
[13] A. Iserles, *A first course in the numerical analysis of differential equations*. Cambridge university press, 2009, no. 44.